



Propylene oxide ring opening with aniline: a combined experimental and DFT theoretical calculation study

Sajad Asadbegi^{1*}, Manoochehr Farzin¹, Keyvan Nostarzedegan¹, Mohammad Ferdosi²

¹Department of Material Science and Engineering, Malek-ashtar University of Technology, Shahin-shahr, Isfahan, (IRAN)

²Chemistry and Chemical Engineering Research Centre of Iran, Tehran, (IRAN)

E-mail: sajad.asadbegi@gmail.com

ABSTRACT

The nucleophilic ring opening of epoxides with amines is a famous pathway for the synthesis of β -amino alcohols. In this work, the reaction of propylene oxide with aniline in presence of LiBr as a catalyst without using solvent is reported and the reaction products characterized by elemental analysis, ¹H, ¹³C NMR, and FT-IR spectroscopy. The molecular geometry of products and intermediates have been calculated by using density functional methods (B3LYP) with 6-311++G(d,p) as basis set. The variation of dipole moments of major product, NBO charges on atoms in the gas phase and the thermodynamic properties of reaction were studied.

© 2015 Trade Science Inc. - INDIA

KEYWORDS

Epoxide ring opening;
 β -amino alcohols;
 Density functional theory;
 Thermodynamic studies.

INTRODUCTION

Epoxides are important molecules because of their importance as highly useful precursors for the synthesis of organic compounds. They are able to react with several nucleophiles, which their action of epoxides with amines due to the formation of β -amino alcohols is specifically interesting^[1-3]. The epoxide ring opening by amines is the key step for the preparation of new therapeutic agents, unnatural amino acids^[4-5], chiral auxiliaries^[3], and biologically active compounds of synthetic and natural source^[6-9]. β -amino alcohols are compounds of undisputed interest in synthetic organic chemistry being found as subunits in many important biologically active synthetic and natural products. Furthermore, the amino alcohol moieties are essential substructures in

asymmetric synthesis. It has been extensively recognized that enantiopure β -amino alcohols are chiral auxiliaries and valuable ligands in a number of asymmetric organic transformations^[10-11]. The numerous limitations like the necessity of elevated temperature and an excess of amines, undesired side reactions such as polymerization or rearrangement with sensitive epoxides, failure with less/poor nucleophilic and sterically hindered amines, deficiency of appreciable regioselectivity, etc. associated with the classical approach of heating the mixture of epoxide and amine led to the development of various catalytic procedures^[12-21]. This paper discusses the synthesis of β -amino alcohols by ring opening of propylene oxide with aniline in presence of LiBr as a Lewis acid. The ring opening reaction catalyzed by LiBr has been studied by means of DFT (B3LYP)

calculations and the molecular geometry of products and intermediates have been calculated by using density functional methods.

RESULTS AND DISCUSSION

General method

The commercially available reagents were used as received without further purification. The reaction was performed under a nitrogen atmosphere. Nuclear magnetic resonance spectra were recorded on a Bruker Avance 400 (^1H NMR: 400 MHz, ^{13}C NMR: 100 MHz) spectrometer in CDCl_3 at room temperature. Chemical shift values (δ) are given in parts per million using residual solvent protons (^1H NMR: $\delta\text{H} = 7.18$ for CDCl_3 , ^{13}C NMR: $\delta\text{C} = 77.0$ for CDCl_3) as internal standard. The FT-IR spectrum of the samples was recorded on a Unicom Galaxy Series FT-IR 5000 spectrophotometer in the region 4000–500 cm^{-1} using pressed KBr discs.

General procedure

Under nitrogen atmosphere 461.74 g Aniline and 2.2 g lithium bromide were added to a reactor. The mixture was heated to about 80 °C and 4.44 atm under nitrogen atmosphere. Then 820.96 g propylene oxide was added to reaction mixture, which was flowed at a temperature of 125 °C under a pressure of 7.65 atm for 3 h. The reaction mixture was again stirred at 125 °C for 2.5 h. In the last process step, excess of propylene oxide was separated by high temperature and low pressure at 130 °C and 0.75 atm for 1 h. The mixture was purified by using a silica gel (Merck 230–400 mesh) column chromatography with n-hexane:ethyl acetate (6:4, v/v) as the developing solvent.

1,1'-*l*-(phenylazanediyl)bis(propan-2-ol)(AA)

Yellow oil, yield: 58 %. IR (KBr) ν 695, 748, 1038, 1079, 1130, 1236, 1296, 1374, 1504, 1598, 2899, 2928, 2969, 3313 cm^{-1} . ^1H NMR (400.1 MHz, CDCl_3) δ 1.11 (d, J 5.6 Hz, 6H, 2CH_3), 2.90 (d, J 6.8 Hz, 2H, CH_2), 3.11 (d, J 6.8 Hz, 2H, CH_2), 3.97–4.07 (m, 2H, 2CH), 6.69 (d, J 8.8 Hz, 2H, Ar), 6.77–6.80 (m, 1H, Ar), 7.10–7.14 (m, 2H, Ar). ^{13}C NMR

(100.6 MHz, CDCl_3) δ 20.3 (2CH_3), 60.0 (2CH_2), 64.9 (2CH), 112.2 (CH-Ar), 117.4 (CH-Ar), 129.1 (CH-Ar), 149.2 (C-Ar). Anal. Calcd for $\text{C}_{12}\text{H}_{19}\text{NO}_2$: C 68.87, H 9.15, N 6.69. Found: C 68.92, H 9.23, N 6.64.

2-((2-hydroxypropyl)(phenylamino)propan-1-ol AB(=BA))

Yellow oil, yield: 27 %. IR (KBr) ν 695, 748, 1001, 1038, 1078, 1128, 1240, 1375, 1504, 1597, 1628, 1654, 2925, 2968, 3247 cm^{-1} . ^1H NMR (400.1 MHz, CDCl_3) δ 1.17 (2d, J 6.4 Hz, 6H, 2CH_3), 2.75–2.80 (m, H, CH), 2.90–2.94 (m, 2H, CH_2), 3.44–3.59 (m, 2H, CH_2), 3.77–3.80 (m, H, CH), 6.56–6.74 (m, 2H, Ar), 6.75 (m, 1H, Ar), 7.10–7.18 (m, 2H, Ar). ^{13}C NMR (100.6 MHz, CDCl_3) δ 14.2 (CH_3), 19.5 (CH_3), 59.8 (CH), 64.0 (CH_2), 66.2 (CH_2), 64.7 (CH), 112.6 (CH-Ar), 117.2 (CH-Ar), 129.3 (CH-Ar), 151.2 (C-Ar). Anal. Calcd for $\text{C}_{12}\text{H}_{19}\text{NO}_2$: C 68.87, H 9.15, N 6.69. Found: C 68.85, H 9.18, N 6.76.

2,2'-*l*-(phenylazanediyl)bis(propan-1-ol) (BB)

Yellow oil, yield: 9 %. IR (KBr) ν 696, 750, 1051, 1316, 1374, 1602, 2980, 3035, 3292 cm^{-1} . ^1H NMR (400.1 MHz, CDCl_3) δ 1.24 (d, J 7.2 Hz, 6H, 2CH_3), 2.75–2.83 (m, 2H, 2CH), 3.53–3.58 (m, 2H, CH_2), 3.76–3.80 (m, 2H, CH_2), 6.64–6.79 (m, 2H, Ar), 6.80–6.84 (2, H, Ar), 7.08–7.12 (t, J 8 Hz, 2H, Ar). ^{13}C NMR (100.6 MHz, CDCl_3) δ 17.5 (2CH_3), 51.7 (2CH), 66.2 (2CH_2), 113.3 (CH-Ar), 117.9 (CH-Ar), 129.3 (CH-Ar), 148.2 (C-Ar). Anal. Calcd for $\text{C}_{12}\text{H}_{19}\text{NO}_2$: C 68.87, H 9.15, N 6.69. Found: C 68.83, H 9.19, N 6.72.

Computational details

Theoretical calculations were accomplished using GAUSSIAN 09 package and the Gauss-View molecular visualization program²² on a personal computer. The geometry optimization of the title compound and corresponding energy and harmonic vibrational frequencies were calculated at level of theories with 6-311++G(d,p) basis set by assuming Cs point group symmetry. The absence of imaginary frequency verified that optimized geometry for the title molecule was true minima on the potential energy surface at their respective levels of theory. The

Full Paper

natural bond orbital (NBO) technique was performed on the optimized structures at B3LYP/6-311++G(*d,p*) level^[23]. The effect of one LiBr molecule in presence of the compounds was considered at B3LYP/6-311++G(*d,p*) method. As a result, the optimized geometrical parameters, energy, fundamental vibrational frequencies, the atomic charges, dipole moments and other thermodynamical parameters were calculated theoretically.

Molecular geometry

The molecular structures were optimized by DFT method. The results of calculated total energies (Hartree), relative stabilities (kcal/mol) of structures are collected in TABLE 1 and 2, respectively. The results of calculations show that AB (=BA) is the most stable product in order of $AB \geq AA > BB$ in the gaseous phase by 0.15 and 9.67 kcal/mol, respectively (1 cal=4.184 J). The difference between AB and BA is with which oxygen LiBr is interacting. It is notable that based on DFT calculations, AA is the most stable structure in presence of one LiBr molecule and the order of stability of structures are $AA > AB > BB > BA$ by 0.74, 8.14 and 12.02 kcal/mol, respectively, that is the same as the order of the yielded obtained product. The stability of A and B intermediates²⁴⁻²⁵ was not affected in presence of one LiBr molecule and A is most stable than B. The results of calculated relative energies and dipole moments of optimized structures at B3LYP levels using

6-311++G(*d,p*) basis function are presented in TABLE 3. A close look at TABLE 3 shows that order of dipole moments is $AA > BB > AB$ in the gas phase and $BB > AA > BA > AB$ in presence of one LiBr molecule in the gas phase. The order of dipole moments of A and B intermediates was not changed. The most stable structures of AA and AA...LiBr with numbering of the atoms is shown in Figure 1. The optimized values of bond lengths are reported in TABLE 4.

Charge distribution

The calculated values of NBO charges by natural population analysis (NPA) of optimized structure of AA in the gas phase are given in TABLE 5. It can be seen that in the gas phase, the O33, C11 and C26 positions carries most negative charge. In the AA...LiBr compounds when LiBr complexed to AA, the Br36 and O33 atoms have the most negative charge. According to the NBO results, O11 doe to coordinated to Li has the most change in negative charge.

Thermodynamic properties

The prognostication of reaction kinetics and the behavior of organic compounds need a perfect description of their thermochemical properties. According to the second law of thermodynamics in thermochemical field, the thermodynamic data supply helpful information to evaluate the amount of

TABLE 1 : Total energies (Hartree) and relative stabilities (kcal/mol) at DFT 6-311G++(*d,p*) in the gas phase

structures		A	B	
intermediates	Total energies	-480.8980749	-480.8953777	
	Relative stabilities	0	1.69	
structures		AA	AB (=BA)	BB
products	Total energies	-674.0993381	-674.0995768	-674.0841635
	Relative stabilities	0.15	0	9.67

TABLE 2 : Total energies (Hartree) and relative stabilities (kcal/mol) at DFT 6-311G++(*d,p*) in the gas phase with one LiBr molecule

structures		A		B	
intermediates	Total energies	-3062.70064		-3062.69797	
	Relative stabilities	0.00		1.68	
structures		AA	AB	BA	BB
products	Total energies	-3255.89666	-3255.89390	-3255.87750	-3255.88368
	Relative stabilities	0.00	1.74	12.02	8.14

TABLE 3 : Calculated dipole moments of optimized structures

structures		A		B	
intermediates	Total energies	1.96		2.29	
	Relative stabilities	7.58		8.34	
structures		AA	AB	BA	BB
products	Total energies	4.23	2.78	2.78	3.04
	Relative stabilities	11.43	9.56	11.78	13.35

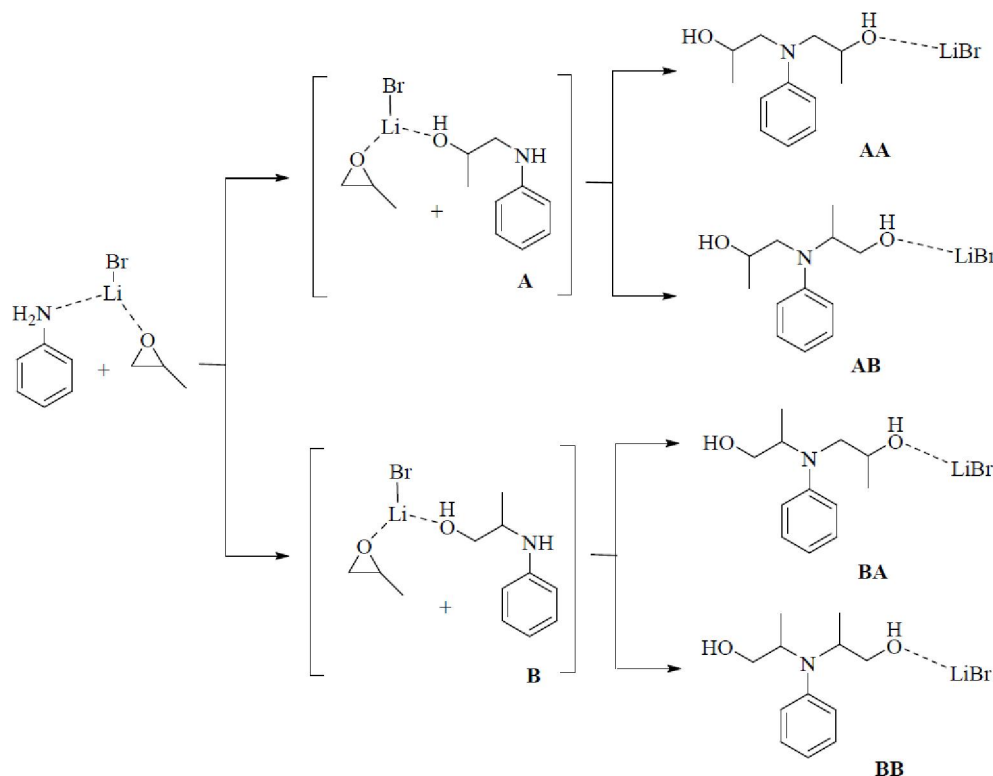


Figure 1: Synthetic route for AA, AB (=BA) and BB in presence of LiBr

energy released or absorbed in a chemical reaction and to calculate other thermodynamic functions, such as Gibbs energies and equilibrium constants, and more importantly, they permit a quantitative assessment of the relative stability of a molecule^[26]. On this subject, estimation methods, ab initio quantum mechanical methods, and more recently, density functional theory (DFT) calculations, often because of lack of available experimental data, have been used as an independent confirmation of the accuracy of the experimental measurement. In the current study, the thermodynamic data for the reactants and products in the reaction at B3LYP levels using 6-311++G(d, p) basis function are given in the TABLE 6. According to the result, at standard ambient temperature and

pressure, the A intermediate is thermodynamically favorable. This result also has been obtained on the reaction conditions (398.15 K, 7.65 atm). Therefore, in the first step of the reaction the A intermediate is the more thermodynamically stable and will produce extra than B. In the second step of the reaction, the concentrations of A and B intermediates are determinants which the final product would extra produce. From A intermediate AA and AB products were obtained as well as BA and BB from B intermediate. It is reasonable to assume that AA and AB products from thermodynamically favorable A intermediate, were the major product. At standard ambient temperature and pressure and on the reaction conditions (398.15 K, 7.65 atm), AA is more thermodynamically favorable than AB, but the re-

TABLE 4 : Calculated optimized parameter values of a and b.

Bond Label	Bond Length (Å)		Bond Label	Bond Length (Å)	
	(a)	(b)		(a)	(b)
C1-H12	1.082	1.082			
C2-H13	1.085	1.085	C2-C3	1.392	1.391
C3-H14	1.084	1.084	C3-C4	1.395	1.395
C4-H15	1.085	1.085	C4-C5	1.390	1.390
C5-H16	1.083	1.083	C5-C6	1.408	1.406
C8-H17	1.101	1.101	C6-C1	1.406	1.404
C8-H18	1.092	1.092	C8-C9	1.551	1.549
C9-H19	1.098	1.098	C9-C10	1.522	1.519
C10-H20	1.092	1.092	C30-C24	1.533	1.533
C10-H21	1.094	1.094	C24-C25	1.527	1.525
C10-H22	1.094	1.094	C9-O11	1.420	1.446
C30-H31	1.104	1.104	C24-O33	1.435	1.441
C30-H32	1.090	1.090	N7-C6	1.411	1.418
C24-H25	1.098	1.098	N7-C8	1.464	1.462
C25-H27	1.094	1.094	N7-C30 O33.H23*	1.452	1.455
C25-H28	1.094	1.094	Li-O11	2.256	1.997
C25-H29	1.093	1.093	Li-Br	-	1.876
C1-C2				-	2.232

* Intramolecular H bond lengths

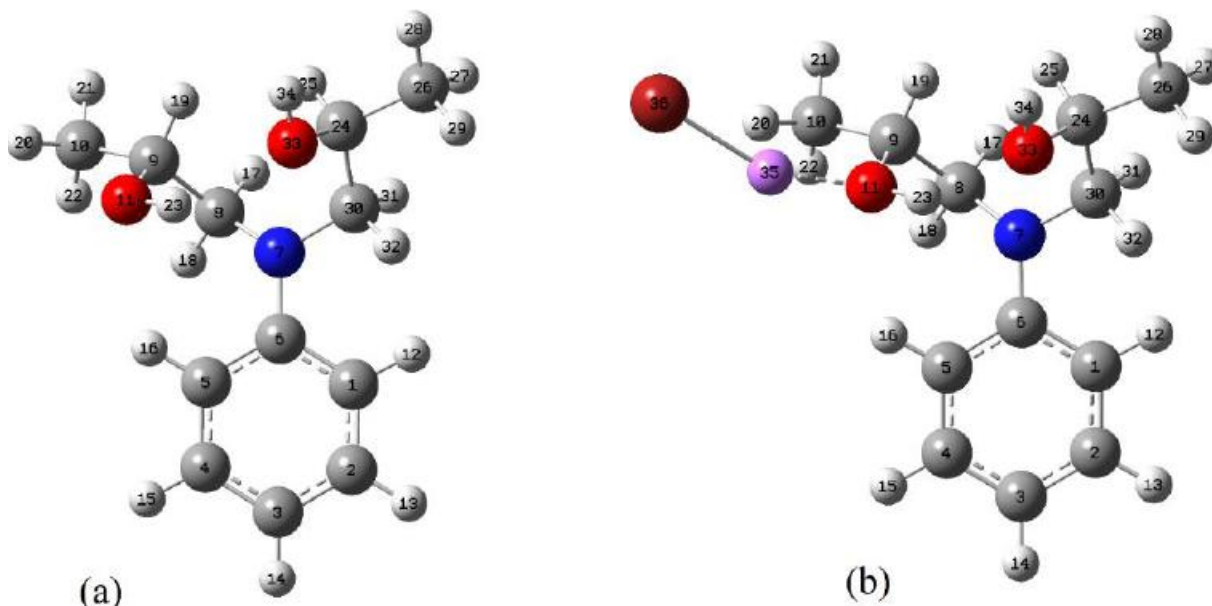


Figure 2 : (a) Molecular structure of AA; (b) Molecular structure of AA...LiBr along with numbering of atoms

lation between BA and BB products are changing with increase of temperature and pressure. At standard ambient temperature and pressure BA is more thermodynamically favorable than BB, while with increasing temperature and pressure an inverse relationship has been seen. There are two routes re-

action for obtain AB (=BA) from A and B intermediate, so. It is reasonable to assume that this product is obtained more than BB. By comparing the yield of product and the theoretical thermodynamic data, the highly suitable agreement between theoretical and experimental result was appreciated.

TABLE 5 : Calculated NBO charges on atoms of (a) and (b) structures in the gas phase

Atom	Tautomer		Bond Label	Tautomer	
	(a)	(b)		(a)	(b)
C1	-0.26	-0.25	H19	0.14	0.16
C2	-0.19	-0.18	H20	0.21	0.23
C3	-0.24	-0.23	H21	0.20	0.22
C4	-0.19	-0.18	H22	0.20	0.21
C5	-0.25	-0.25	H23	0.49	0.52
C6	0.19	0.19	C24	0.11	0.11
N7	-0.53	-0.54	H25	0.15	0.15
C8	-0.19	-0.18	C26	-0.60	-0.60
C9	0.11	0.12	H27	0.21	0.21
C10	-0.59	-0.60	H28	0.20	0.21
O11	-0.76	-0.82	H29	0.21	0.21
H12	0.20	0.20	C30	-0.17	-0.18
H13	0.20	0.20	H31	0.18	0.18
H14	0.20	0.21	H32	0.21	0.21
H15	0.20	0.21	O33	-0.75	-0.76
H16	0.23	0.21	H34	0.46	0.47
H17	0.17	0.19	Li35	-	0.71
H18	0.21	0.21	Br36	-	-0.78

TABLE 6 : Theoretical thermodynamic data (Kcalmol⁻¹) of reaction product in the gas phase

		A	B	AA	AB	BA	BB
298.15 K, 101325 pa	ΔH	-16.72	-14.98	-7.66	1.18	-7.97	1.43
	ΔG	-12.90	-10.96	-4.06	4.35	-4.32	1.23
398.15 K, 775136 pa	ΔH	-16.89	-15.18	-7.81	1.06	10.42	1.36
	ΔG	-11.59	-9.57	-2.83	5.43	15.53	0.55

it is the major product in the experiment reaction.

CONCLUSION

In summary, the reaction of propylene oxide ring opening with aniline was performed and the reaction products was characterized by elemental analysis, ¹H, ¹³C NMR, and FT-IR spectroscopy. The DFT calculations show that AA is the most stable structure in presence of one LiBr molecule as catalyst in the gas phase, and that there is a suitable agreement between theoretical and experimental result. The charges of atoms in major product (AA) and in presence of one molecule LiBr as catalyst (AA...LiBr) were calculated by NBO method in gas phase. Based on the obtained thermodynamical data, on the reaction conditions (398.15 K, 7.65 atm), AA is more thermodynamically favorable than other products so

REFERENCES

- [1] E.J.Corey, F.Zhang; *Angew.Chem., Int.Ed.***38**, 1931-1934 (1999).
- [2] C.W.Johannes, M.S.Visser, G.S.Weatherhead, A.H.Hoveyda, *J.Am.Chem.Soc.*,**120**, 8340-8347 (1998).
- [3] D.J.Ager, I.Prakash, D.R.Schaad; *Chem.Rev.*, **96**, 835-876 (1996).
- [4] P.O'Brien; *Angew.Chem., Int.Ed.***38**, 326-329 (1999).
- [5] G.Li, H.T.Chang, K.B.Sharpless; *Angew.Chem., Int.Ed.*,**35**, 451-454 (1996).
- [6] E.Ruediger, A.Martel, N.Meanwell, C.Solomon, B.Turmel; *Tetrahedron Lett.*, **45**, 739-742 (2004).
- [7] A.Sekine, T.Ohshima, M.Shibasaki; *Tetrahedron*, **58**, 75-82 (2002).

Full Paper

- [8] X.L.Hou, J.Wu, L.X.Dai, M.H.Tang; *Tetrahedron: Asymmetry*, **9**, 1747-1752 (1998).
- [9] J.Lieoscher, S.Jin, A.Otto; *J.Heterocycl.Chem.*, **37**, 509-518 (2000).
- [10] Anandkumar B.Shivarkar, Sunil P.Gupte, Raghunath V.Chaudhari; *Ind.Eng.Chem.Res.*, **47(8)**, 2484-2494 (2008).
- [11] Satoshi Horii, Hiroshi Fukase, Takao Matsuo, Yukihiko Kameda, Naoki Asano, Katsuhiko Matsui; *J.Med.Chem.*, **29**, 1038-1046 (1986).
- [12] T.Ollevier, G.Lavie-Compin, *Tetrahedron Lett.*, **45**, 49-52 (2004).
- [13] P.Q.Zhao, L.W.Xu, C.G.Xia; *Synlett.*, 846-850 (2004).
- [14] A.McCluskey, S.K.Leitch, J.Garner, C.E.Caden, T.A.Hill, L.R.Odell, S.G.Stewart; *Tetrahedron Lett.*, **46**, 8229-8232 (2005).
- [15] A.T.Placzek, J.L.Donelson, R.Trivedi, R.A.Gibbs, S.K.De; *Tetrahedron Lett.*, **46**, 9029-9034 (2005).
- [16] D.B.Williams, M.Lawton; *Tetrahedron Lett.*, **47**, 6557-6560 (2006).
- [17] S.Bonollo, F.Fringuelli, F.Pizzo, L.Vaccaro; *Synlett*, 2863-2867 (2007).
- [18] R.I.Kureshy, S.Singh, N.H.Khan, S.H.R.Abdi, E.Suresh, R.V.Jasra; *J.Mol.Catal.A: Chem.*, **264**, 162-169 (2007).
- [19] M.J.Bhanushali, N.S.Nandurkar, M.D.Bhor, B.M.Bhanage; *Tetrahedron Lett.*, **49**, 3672-3676 (2008).
- [20] R.Chakravarti, H.Oveisi, P.Kalita, R.R.Pal, S.B.Halligudi, M.L.Kantam, A.Vinu; *Microporous Mesoporous Mater*; **123**, 338-344 (2009).
- [21] A.Bordoloi, Y.K.Hwang, J.S.Hwang, S.B.Halligudi; *Catal.Comm.*, **10**, 1398-1403 (2009).
- [22] Mjea Frisch, G.W.Trucks, Hs B.Schlegel, G.E.Scuseria, M.A.Robb, J.R.Cheeseman, G.Scalmani, V.Barone, B.Mennucci, G.A.Petersson; Gaussian 09, Revision A.02, Gaussian.Inc., Wallingford, CT, **200**, (2009).
- [23] Natalia V.Belkova, Tatyana N.Gribanova, Evgenii I.Gutsul, Ruslan M.Minyaev, Claudio Bianchini, Maurizio Peruzzini, Fabrizio Zanobini, Elena S.Shubina, Lina M.Epstein; *J.Mol.Struc-Theochem*, **844-845 (0)**, 115-131 (2007).
- [24] Brahmam Pujala, Shivani Rana, Asit K.Chakraborti; *JOC* 2011, **76(21)**, 8768-8780.
- [25] Nianyuan Tan, Shuangfeng Yin, Yuefang Li, Renhua Qiu, Zhengong Meng, Xingxing Song, Shenglian Luo, Chak-Tong Au, Wai-Yeung Wong; *J.Organomet.Chem.*, **696(8)**, 1579-1583 (2011).
- [26] J.B.Ott, J.Boerio-Goates; *Chemical Thermodynamics: Advanced Applications: Advanced Applications*.Elsevier Science: (2000).